Background correlations selectively boost the gamma-sensitivity of cortical GABAergic neurons

Ricardo Martins Merino[1,2,3,4,5], Carolina Leon-Pinzon[1,2,3,5], Walter Stühmer[3,5], Martin Möck[6], Jochen F. Staiger[6], Fred Wolf[1,2,3,5,7,8], Andreas Neef[1,2,3,5,7,8*†]

[1]Max Planck Institute for Dynamics and Self-Organization, Am Faßberg 17, 37077 Göttingen, Germany
[2]Campus Institute for Dynamics of Biological Networks, Hermann Rein St. 3, 37075 Göttingen, Germany
[3]Bernstein Center for Computational Neuroscience Göttingen, Germany
[4]Göttingen Graduate Center for Neurosciences, Biophysics, and Molecular Biosciences, University of Göttingen, Germany
[5]Max Planck Institute of Experimental Medicine, Hermann Rein St. 3, 37075 Göttingen, Germany
[6]Institute for Neuroanatomy, University Medical Center Göttingen, Georg-August-University, Göttingen 37075, Germany
[7]Institute for Nonlinear Dynamics, Georg-August University School of Science, Friedrich Hund Pl. 1, 37077 Göttingen, Germany
[8]Center for Biostructural Imaging of Neurodegeneration, Von-Siebold-St. 3A, 37075 Göttingen, Germany.
[*]e-mail: aneef@gwdg.de †lead author

SUMMARY

Gamma oscillations in cortical circuits critically depend on GABAergic interneurons. Precisely which interneuron types and populations can drive cortical gamma, however, remains unresolved and may depend on brain state. Here we show that spike-frequency adapting interneurons dramatically boost their gamma-sensitivity in the presence of slowly fluctuating background activity. This mechanism allows the dynamic control of gamma oscillations, induces cross-frequency coupling and predicts these interneurons to be exquisitely sensitive to high-frequency ripples.

INTRODUCTION

Collective rhythmic activity is implicated in brain functions from sensory information processing to memory consolidation and depends on the interplay between inhibitory and excitatory neuronal populations[1, 2]. Fast-spiking (FS), parvalbumin-positive interneurons are closely associated with the initiation and maintenance of gamma oscillations (30-150 Hz)[3, 4]. When driven with frequency chirps, and as a result of intrinsic membrane properties, FS neurons fire more robustly at higher input frequencies than spike-frequency adapting (AD), somatostatin-positive interneurons, which are most responsive to lower frequencies[5]. Nevertheless, recent studies strongly suggest that, under certain conditions, somatostatin-positive interneurons are crucial for gamma oscillations[6, 7]. Could the spectral sensitivity of different interneuron populations perhaps be itself state-dependent? Here we characterized the spectral sensitivity of cortical GABAergic interneurons at different *in vivo*-like working points by measuring their dynamic gain[8-12]. Dynamic gain quantifies how input in different frequency bands modulates population firing under *in vivo*-like conditions of fluctuating background input. To probe the potential impact of different brain states on spectral sensitivity, we used different types of background inputs that mimic the strength and timescales of correlations in background input across brain states[13]. We find that both FS and AD interneuron populations have remarkably wide bandwidths (up to about 500 Hz), making them capable of tracking fast input frequencies well into the range of sharp wave-ripples. Moreover, our results uncover an unanticipated flexibility in AD neurons, which can massively shift their frequency preference. In particular in the presence or absence of slowly-correlated input, such as during slow wave sleep or active wakefulness respectively, AD neurons specifically engage or disengage with high frequency rhythms, such as gamma and sharp wave-ripples.

RESULTS

AD and FS (Figures 1A and 1B) are the most common firing patterns of somatostatin- and parvalbumin-positive interneurons, respectively[14]. Their spectral selectivity has been investigated through sub- and supra-threshold cellular responses to simple, purely sinusoidal inputs[5] (Figures 1C and 1D). However, *in vivo* even when activity on the population level is periodic, the firing of individual neurons appears stochastic, driven by noisy,

fluctuating inputs rather than pure sinusoids[11, 15]. We thus probed the spectral sensitivity of mouse layer 2/3 prefrontal FS and AD interneuron populations under naturalistic operating conditions (Figure 1E). To this end, we determined their dynamic gain under two different regimes of fluctuating input, distinguished by the correlation time τ: the first case, τ = 5 ms (Figure 1E, black traces), mimics the case of completely asynchronous population activity, when the decay time-constant of synaptic currents is the only source of input correlations. The other input, characterized by a much slower 25 ms correlation time (Figure 1E, gray traces), mimics brain states with population activity exhibiting slow fluctuations, such as quiet wakefulness[13].

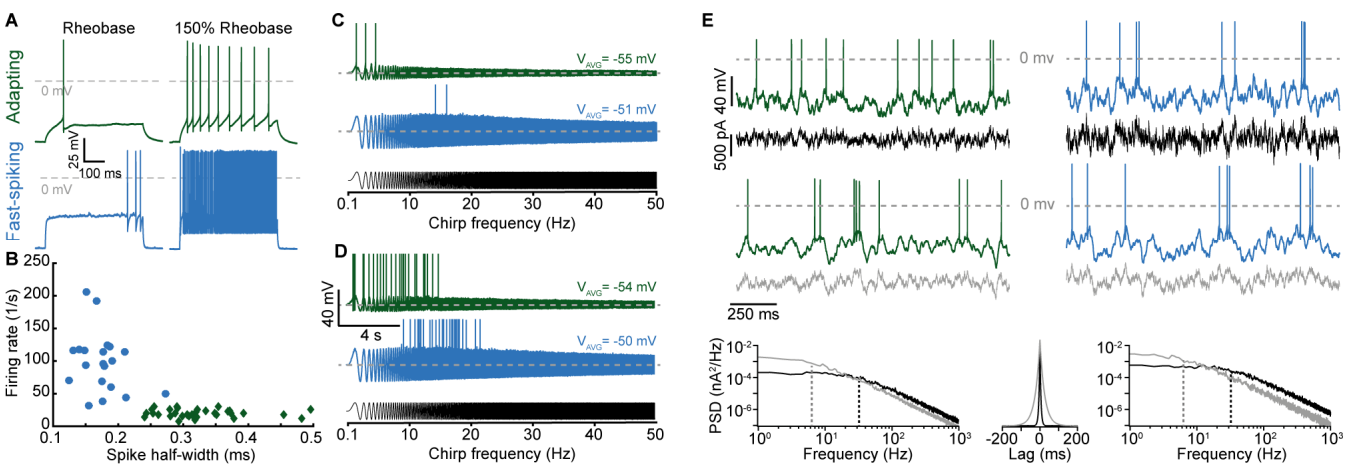

Figure 1. Characterization of neocortical adapting and fast-spiking interneurons. (A) Square pulses of 500 ms were used to determine the recorded neuron's firing pattern at the 150% rheobase level. Shown are representative responses of adapting (AD, green) and fast-spiking (FS, blue) neurons at rheobase and 150 % rheobase. (B) Spike half-width and firing rate allow a clear distinction between these cell types. (C) Frequency chirp currents (black) have been used to characterize the spectral sensitivity of neurons. They yield action potentials (shown clipped) at lower input frequencies for AD neurons than for FS neurons. (D) A slight increase in the offset current, resulting in only a 1 mV depolarization, results in overlapping bandwidths for AD and FS neurons, indicating substantial uncertainty in chirp-based characterizations. (E) We assessed neuronal encoding performance in two *in vivo*-like regimes, distinguished by the correlation time of the fluctuating stimuli (τ = 5 ms, black, and τ = 25 ms, gray). The amplitude of the stimulus at each trial was adjusted to achieve a target operating point (characterized by firing rate and spike train irregularity; see Methods). The corresponding voltage traces of AD and FS neurons are shown above the stimuli, and the power spectral densities (PSDs) as well as the amplitude-normalized autocorrelations of the inputs are shown at the bottom. The dashed lines in the PSDs indicate the cut-off frequencies (32 Hz and 6.4 Hz) corresponding to the correlation times of the different inputs.

The spectral sensitivity of interneurons was markedly different from their chirp responses and for AD cells changed drastically between the two conditions (Figure 2A). In the asynchronous regime, AD neurons respond preferentially to slow components, with highest sensitivity in the 2-4 Hz range (mean = 119 Hz/nA, 95% bootstrap confidence interval: [117, 122]). The average gain in the gamma range (Figure 2A, shaded region) reaches only 63% of the average at lower frequencies (< 20 Hz) (65 Hz/nA [63, 66] vs 103 Hz/nA [101, 105]). These values mean that the addition of a small, 10 pA sinusoidal modulation (equivalent in magnitude to a single synaptic event) on top of the irregularly fluctuating background input would modulate AD population's firing rate by 1.2 Hz in response to an superimposed 3 Hz input, but it would modulate the firing rate only by 0.6 Hz for 60 Hz, indicating a clear preference for lower frequencies. This preference, however, changed completely when AD neurons were exposed to slowly fluctuating input such that their preferred frequency shifted from 3 Hz to 200 Hz. The gain at 2-4 Hz dropped from 119 Hz/nA [117, 122] to 91 Hz/nA [89, 92], and the gain at 200 Hz increased from 74 Hz/nA [72, 76] to 119 Hz/nA [113, 124]. Figure 2B demonstrates the occurrence of this shift in individual AD neurons. With this abrupt change in frequency preference, AD neurons in the synchronous regime become more sensitive to gamma input than to lower frequencies (average gains: 94 Hz/nA [91, 98] vs 81 Hz/nA [80, 83]). Altogether, these data reveal that, during network states characterized by slow background fluctuations, AD cells tune themselves to gamma and higher-frequency input. FS interneurons, on the other hand, preferentially transmit high frequencies irrespective of the input correlations, with a maximum sensitivity around 200-250 Hz (Figure 2C). Both FS and, given sufficiently slow input components, AD interneurons have a remarkably wide bandwidth, with a high frequency limit well above 400 Hz an order of magnitude higher than expected from their chirp-responses.

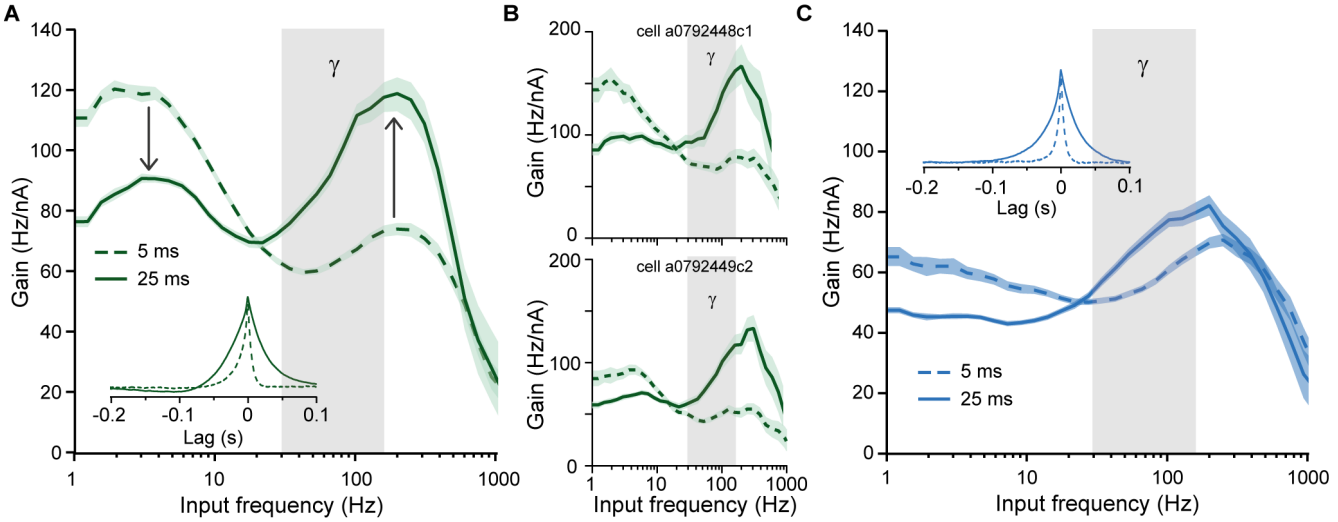

Figure 2. Spectral selectivity of AD neurons drastically shifts for different background fluctuations. (A) AD neurons were driven with inputs of different correlation times. Under fast background, τ = 5 ms (dashed lines, n = 12), AD neurons modulate their firing rate strongest in response to lower frequencies. Under slow background, τ = 25 ms (continuous line, n = 10), the frequency preference shifts (arrows) and the firing rate is modulated mainly by high frequencies. Mean firing rate and coefficient of variation of the interspike intervals were 4.0 Hz ± 0.2 and 0.99 ± 0.02 (5 ms input) and 3.7 Hz ± 0.2 and 1.03 ± 0.05 (25 ms input), respectively. Inset: spike-triggered average input across all recorded cells tested with the same correlation times. Gains were calculated by taking the ratio of the Fourier transforms of the spike-triggered average and of the autocorrelation function of the input. Gray columns represent the gamma frequency-band and the shaded region around gain curves represents the 95% bootstrap confidence interval. (B) Individual gain curves of the two AD cells from (A) for both correlation times. The drastic shift in frequency preference is clearly visible at the single-cell level. (C) As in (A), but for FS neurons, which display no drastic shifts in frequency preference (τ = 5 ms, dashed lines, n = 7; τ = 25 ms, continuous lines, n = 9). Grand-averaged firing rate and coefficient of variation of the interspike intervals were 5.0 Hz ± 0.6 and 1.12 ± 0.24 (5 ms) and 3.6 Hz ± 0.2 and 1.47 ± 0.10 (25 ms). Numbers given as mean ± SEM.

This input-dependent spectral sensitivity might allow AD neurons to provide state-dependent feedback input into the local cortical circuit. Interestingly, AD neurons shift their preference to the gamma-band when their input is dominated by lower frequencies. This suggests that, the presence of theta oscillations (4-12 Hz) could tune them to higher frequencies, boosting gamma components. To test this hypothesis, we exposed AD neurons to the rapidly fluctuating, 5 ms correlated background input, either on its own or supplemented with theta-band components (Figure 3A). We found that the theta-band components in fact boosted the gain for frequencies above 30 Hz, with the average gamma-band gain increasing from 73 Hz/nA [71, 75] to 86 Hz/nA [83, 89] (Figure 3B). The gamma/theta ratio increased in 9 out of 10 cells, from 0.58 ± 0.02 to 0.74 ± 0.04 (mean ± SEM; Figure 3C), revealing that, indeed, an increase in theta power boosts gamma sensitivity of AD neurons.

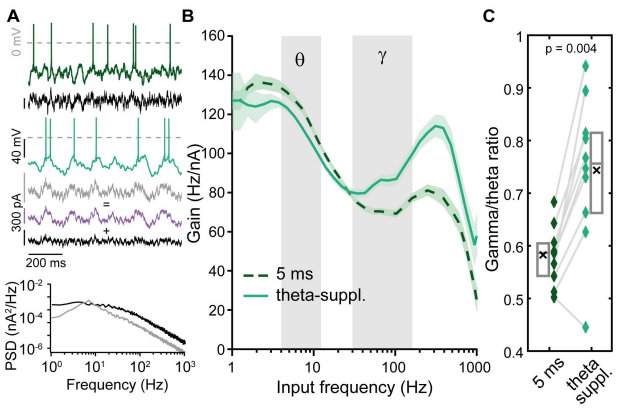

Figure 3. Increasing theta input to AD neurons boosts sensitivity to gamma and high-frequencies. (A) Sample stimuli and voltage traces (dark green, 5 ms input; light green, theta-supplemented input) and power spectral density of noisy inputs with τ = 5 ms (black) and theta-supplemented 5 ms input (gray). Theta-supplemented input was constructed by adding a theta band-pass filtered white noise input (purple) to the 5 ms input. Grand-averaged firing rate and coefficient of variation of the interspike intervals were 4.58 Hz ± 0.23 and 0.97 ± 0.03 (5 ms input) and 4.78 Hz ± 0.26 and 0.92 ± 0.04 (theta-supplemented 5 ms input). (B) Gain of AD cells tested with both, τ = 5 ms (dashed line) and theta-supplemented 5 ms (continuous line) inputs (n = 10). Boosting theta promotes sensitivity to gamma and higher frequencies. (C) Frequency-band preference was obtained from the ratio between the average gains at gamma (30-150 Hz) and theta (4-12 Hz) bands. Gamma/theta ratio increases by adding theta-power to the input (τ = 5 ms: 0.58 ± 0.02 vs theta-supplemented 5 ms: 0.74 ± 0.04, n = 10. Two-sided Wilcoxon signed rank test, W = 1, p = 0.004). Box plots show mean (black cross), median and central quartiles. Numbers given as mean ± SEM.

DISCUSSION

In summary, we measured the dynamic gain of FS and AD neurons, which determines their propensity to engage in different brain rhythms. Under fast background fluctuations, as occur during active wakefulness, our data support the traditional picture in which AD neurons preferentially encode low frequency input and FS neurons encode high frequency (>30 Hz) input. When input correlations are slow, however, a drastic change in frequency preference occurs specifically for AD neurons. The finding of such tunable spectral sensitivity reconciles apparently conflicting *in vivo* observations regarding the contribution of AD neurons to gamma oscillations[6, 16]. In particular, our results suggest that the contribution of these interneurons to gamma oscillations is stronger under conditions in which the local field potential features dominant low-frequency components. Our findings thus uncover an unanticipated flexibility of interneuron function.

The increased encoding of high frequencies (>30 Hz) in the presence of strong, slow (theta) components (Figure 3) might be connected to the phenomenon of theta-gamma cross-frequency coupling[17], which, we predict, would be potentiated by AD neurons. In the framework of pyramidal-interneuron network gamma (PING) models[2], input-dependent spectral sensitivity of AD and FS neurons is predicted to increase gamma frequency and amplitude when theta-power is increased. The tuning of spectral sensitivity by background correlations is, to our knowledge, the first mechanism coupling gamma amplitude to theta oscillations that is based on cellular electrophysiological properties.

The wide bandwidth of AD and FS neurons of up to 500 Hz and a maximal sensitivity reached around 200 Hz is by itself a striking phenomenon. In cortical pyramidal neurons high bandwidth dynamic gain is known to mediate the sub-millisecond precision of population coding for input changes[18], but what function could a narrow preference band at around 200 Hz serve? Retrieval and consolidation of episodic memory require a complex and precise replay of activity by cell assemblies in the form of high-frequency sharp wave-ripples (150-300 Hz). Intriguingly, these occur specifically during periods of synchronous network activity, such as during slow-wave sleep or quiet wakefulness[19], when, as we showed, AD and FS neurons are most sensitive to high frequencies. Given the input-dependent selectivity switch in AD neurons, slow oscillations may, in general, boost high-frequency sensitivity of interneurons, and specifically allow AD neurons to tune-in to ripple-related inputs and disinhibit cortical circuits in a precisely timed manner.

ACKNOWLEDGMENTS
This work was supported by the Federal Ministry of Education and Research (BMBF, grant numbers 01GQ1005B, 01GQ1005E), the VW Foundation (ZN2632), by a GGNB Excellence Stipend of the University of Göttingen (R.M.M), and by the Max Planck Society.

AUTHOR CONTRIBUTIONS
R.M.M., C.L.P., F.W., and A.N. conceived the study. R.M.M. performed the experiments with contribution from M.M. R.M.M., C.L.P., F.W., and A.N. analyzed and interpreted the data. F.W., A.N., W.S. and J.F.S provided resources. All authors discussed and interpreted the data. R.M.M., F.W, and A.N. wrote the paper with inputs from all other authors.

DECLARATION OF INTERESTS
Authors declare no competing interests.

METHODS

Animals and slice preparation. All experiments were performed in accordance with institutional and state regulations (Niedersächsisches Landesamt für Verbraucherschutz und Lebensmittelsicherheit). Experiments were performed in 3 to 8-week-old mice of either sex from five different mouse lines. Two lines target mostly AD interneurons: GIN (FVB-Tg(GadGFP)45704Swn, The Jackson Lab #003718) and SOMCrexAi9 (Ssttm2.1(cre)Zjh/J, The Jackson Lab #013044, crossbred with B6.Cg-GT(ROSA)26Sor^tm9(CAG-tdTomato)Hze/J, The Jackson Lab #007909); and three lines target mostly FS interneurons: PVCre[20], PVCrexAi32 (PVCre crossbred with B6;129S-Gt(ROSA)26Sortm32(CAG-COP4*H134R/EYFP)Hze/J, The Jackson Lab # 012569), and Nkx2.1CreERxAi14 (Nkx2-1tm1.1(cre/ERT2)Zjh/J, The Jackson Lab # 014552, crossbred with B6;129S6-Gt(ROSA)26Sortm14(CAG-tdTomato)Hze/J, The Jackson Lab # 007908). Animals were kept in standard 12h light regime with water and food *ad libidum*. Animals were intraperitoneally-injected with a mixture of ketamine and xylazine in PBS (respectively 100 and 20 mg/kg of body weight) and decapitated. The brain was quickly removed and kept in ice-cold, carbogen-saturated cutting solution containing, in mM, 125 NaCl, 2.5 KCl, 26 $NaHCO_3$, 1.25 NaH_2PO_4, 0.4 Ascorbic Acid, 4 Na-Lactate, 25 Glucose, 1 $MgCl_2$, 2 $CaCl_2$ (~315 mOsm, pH 7.4). 300-µm-thick coronal neocortical slices were made in a VT1200S Vibratome (Leica) and incubated at 35°C in carbogen-saturated recording solution (aCSF, in mM: 125 NaCl, 4 KCl, 26 $NaHCO_3$, 10 glucose, 1.3 $MgCl_2$, 2 $CaCl_2$) until recorded.

Patch-clamp recordings. One slice at a time was transferred to a heated recording chamber (PH6 and RC-27L, Warner Instruments) and mechanically-stabilized with a slice hold-down (SHD-27LH/15, Warner Instruments). Throughout the experiment, the slice was gravitationally-perfused with warm aCSF through an in-line heater (HPT-2, Alasciences) at a flow rate of 1-2.5 ml/min. Both the recording chamber and the in-line heater were controlled by a TC-20 temperature controller (NPI electronics). Temperature settings were adjusted so that a target temperature of 36 ± 1° C was measured by a thermistor at the slice position. Slices were visualized in an Axio Examiner.D1 microscope (Zeiss) equipped with a W Plan-Apochromat 40x/1.0 DIC objective. Cells were visualized with infrared differential interference contrast optics (Zeiss) and fluorescent signal was imaged with a multi-wavelength LED source (pE-4000, CoolLed) and a CCD camera (MD061RU-SY, Ximea). 4-6 MOhm pipettes were prepared from borosilicate glass capillaries (PG10165-4, World Precision Instruments) in a vertical puller (PIP 6, HEKA). Internal solution contained, in mM, 135 K-Gluconate, 10 KCl, 4 NaCl, 0.1 Na_4EGTA, 1 Mg-ATP, 0.3 Na-GTP, 10 Hepes, 0.5 Na_2-Phosphocreatine and 0.2% (w/v) biocytin (285-290 MOsm, pH adjusted to 7.3). Whole-cell current-clamp recordings were made in an EPC-10 Double amplifier controlled by Patchmaster (Heka). Fast and slow capacitances and series resistance were carefully adjusted in voltage-clamp mode before recording; fast capacitances while in on-cell configuration, slow capacitances after achieving whole cell. Series resistance was 90-100% compensated with a feedback time-constant of 10 µs. Voltage-signals were low-pass filtered at 8.8 kHz and digitized at 100 kHz. Data analyses were performed in custom-written Matlab 2014b (Mathworks) and Igor Pro 8 (Wavemetrics) programs. Liquid junction potential of -14 mV was not corrected.

Characterization of action potential firing patterns. Layer 2/3 interneurons were identified via fluorescence imaging. In order to identify their electrical type, 500-ms-long 15 pA current steps were injected from resting potential until, at least, a current level 1.5 times larger than rheobase, level at which the characterization of the firing pattern was made. Only cells exhibiting clear fast-spiking (including stuttering cells) and adapting electrical types were included in the analysis.

Dynamic gain calculation. Population frequency-response characterization was restricted to layer 2/3 prefrontal FS and AD interneurons and was assessed as previously described[9, 10]. The goal of this analysis is to achieve an *in vivo*-like operating point, mimicking a situation in which a high rate of synaptic inputs provides a continuously changing net background current, and a neurons' firing is driven not by the average input but by its transient depolarizing excursions[15]. Fluctuating current inputs were synthesized as Ornstein-Uhlenbeck noises $x(t)$ with either 5 or 25 ms correlation times. These values were chosen to approximate the case of uncorrelated inputs filtered through the synaptic currents' decay time-constants (5 ms) or the case of slow temporal correlations in the input due to correlated network activity (25 ms). Inputs' standard deviation was adjusted to obtain similar firing rates (around 4 Hz) and coefficients of variation of the interspike intervals (around 1) across different

conditions. Neurons were first depolarized to -60 mV with DC current and different realizations of the fluctuating noise were injected in 30-s-long episodes, separated by 15-s-long resting, for as long as the recording did not display signs of deterioration, such as baseline drifts or spike overshooting to positive voltages less than 20 mV. For experiments presented in figure 3, a theta-power enhanced stimulus was created by adding a 4-12 Hz band-pass filtered white noise to the 5 ms input. In order to boost the relative contribution of the theta signal to the final input, the standard deviation of the band-pass filtered signal was normalized to two times the standard deviation of the 5 ms signal. In order to obtain the gain curves, spikes were initially detected as 0 mV crossings on the voltage trace and the spike times were annotated. From these, a spike-triggered average (STA) was obtained by summing up 1-s-long stimulus segments centered on the spike times for all cells of a given condition and dividing by the total number of segments. In order to improve signal-to-noise ratio, the STA was filtered in the frequency domain by a Gaussian filter $w(f')$, centered at frequency $f' = f$ and a frequency-dependent window size with standard deviation of$f/2\pi$:

$$w(f') = \frac{1}{\sqrt{2\pi}\left(\frac{f}{2\pi}\right)} exp\left[\frac{-1}{2}\left(\frac{f'-f}{f/2\pi}\right)^2\right]$$

The $STA_w(f)$ thus becomes

$$STA_w(f) = \frac{\int STA(f').w(f').df'}{\int w(f').df'}$$

The dynamic gain $G(f)$ was calculated as the ratio of the Fourier transform of the STA, $F|STA|$, and the Fourier transform of the autocorrelation of the stimulus, $F|c_{ss}(\tau)|$, where

$$c_{ss}(\tau) = \langle x(t)x(t+\tau)\rangle,$$

and τ denotes the time lag. For the dynamic gains reported in figure 2, the data comprise of: for AD neurons, 19563 spikes from 12 cells and 20427 spikes from 10 cells (5 ms and 25 ms respectively), and, for FS neurons, 9792 spikes from 7 cells and 15023 spikes from 9 cells (5 ms and 25 ms, respectively). Five of the 10 AD neurons tested with 5 ms-correlated stimulus were also tested with the theta-supplemented 5 ms input. In addition to these, another 5 were used to obtain the gains in figure 3 (14847 spikes, for 5 ms stimulus and 18067 spikes for theta-supplemented 5 ms stimulus). Confidence intervals were obtained by bootstrap resampling. 500 bootstrapped gain curves were calculated from the same number of STAs obtained by randomly pooling from all STAs used in the population gain calculation. The confidence intervals are defined to be the 2.5th and 97.5th percentiles at each frequency point in the 500 gain curves. The distribution of this bootstrap statistics was not different from normal (Kolmogorov-Smirnov test). To identify the portions of the gain curves that are significantly different from zero, we calculated a noise floor. It was calculated by cyclically-shifting original spike times by a random time interval, larger than 5 correlation times, and calculating 500 “random time-triggered averages”, which were used to calculate “gain curves”. The noise floor was defined as the 95th percentile of these “gain curves”. The gain curves in figures 2 and 3 were displayed either until they were crossed by the noise floor or up to 1000 Hz, if noise floor crossing happened at a frequency > 1000 Hz.

Data availability

All data are available from the corresponding author upon reasonable request. Raw data underlying the dynamic gain curves can be downloaded from this permanent repository at the Max Planck Digital Library: https://edmond.mpdl.mpg.de/imeji/collection/pdxNFpqJurbDDeop.

This permalink is for review purposes. It will be replaced with a DOI.

Code availability

The code, written for IgorPro 8.0, used to analyze raw data and generate the dynamic gain curves is included in the data repository.

REFERENCES

1. Buzsaki, G. & Draguhn, A. Neuronal oscillations in cortical networks. *Science* **304**, 1926-1929 (2004).
2. Cannon, J.*, et al.* Neurosystems: brain rhythms and cognitive processing. *Eur J Neurosci* **39**, 705-719 (2014).
3. Cardin, J.A.*, et al.* Driving fast-spiking cells induces gamma rhythm and controls sensory responses. *Nature* **459**, 663-667 (2009).
4. Whittington, M.A., Traub, R.D. & Jefferys, J.G. Synchronized oscillations in interneuron networks driven by metabotropic glutamate receptor activation. *Nature* **373**, 612-615 (1995).
5. Pike, F.G.*, et al.* Distinct frequency preferences of different types of rat hippocampal neurones in response to oscillatory input currents. *J Physiol* **529 Pt 1**, 205-213 (2000).
6. Veit, J., Hakim, R., Jadi, M.P., Sejnowski, T.J. & Adesnik, H. Cortical gamma band synchronization through somatostatin interneurons. *Nat Neurosci* **20**, 951-959 (2017).
7. Hakim, R., Shamardani, K. & Adesnik, H. A neural circuit for gamma-band coherence across the retinotopic map in mouse visual cortex. *Elife* **7** (2018).
8. Kondgen, H.*, et al.* The dynamical response properties of neocortical neurons to temporally modulated noisy inputs in vitro. *Cereb Cortex* **18**, 2086-2097 (2008).
9. Lazarov, E.*, et al.* An axon initial segment is required for temporal precision in action potential encoding by neuronal populations. *Science advances* **4**, eaau8621 (2018).
10. Higgs, M.H. & Spain, W.J. Conditional bursting enhances resonant firing in neocortical layer 2-3 pyramidal neurons. *J Neurosci* **29**, 1285-1299 (2009).
11. Brunel, N., Chance, F.S., Fourcaud, N. & Abbott, L.F. Effects of synaptic noise and filtering on the frequency response of spiking neurons. *Phys Rev Lett* **86**, 2186-2189 (2001).
12. Naundorf, B., Wolf, F. & Volgushev, M. Unique features of action potential initiation in cortical neurons. *Nature* **440**, 1060-1063 (2006).
13. Poulet, J.F.A. & Crochet, S. The Cortical States of Wakefulness. *Frontiers in systems neuroscience* **12**, 64 (2018).
14. Feldmeyer, D., Qi, G., Emmenegger, V. & Staiger, J.F. Inhibitory interneurons and their circuit motifs in the many layers of the barrel cortex. *Neuroscience* **368**, 132-151 (2018).
15. Destexhe, A., Rudolph, M. & Pare, D. The high-conductance state of neocortical neurons in vivo. *Nat Rev Neurosci* **4**, 739-751 (2003).
16. Chen, G.*, et al.* Distinct Inhibitory Circuits Orchestrate Cortical beta and gamma Band Oscillations. *Neuron* **96**, 1403-1418 e1406 (2017).
17. Canolty, R.T. & Knight, R.T. The functional role of cross-frequency coupling. *Trends Cogn Sci* **14**, 506-515 (2010).
18. Tchumatchenko, T., Malyshev, A., Wolf, F. & Volgushev, M. Ultrafast population encoding by cortical neurons. *J Neurosci* **31**, 12171-12179 (2011).
19. Joo, H.R. & Frank, L.M. The hippocampal sharp wave-ripple in memory retrieval for immediate use and consolidation. *Nat Rev Neurosci* **19**, 744-757 (2018).
20. Meyer, A.H., Katona, I., Blatow, M., Rozov, A. & Monyer, H. In vivo labeling of parvalbumin-positive interneurons and analysis of electrical coupling in identified neurons. *J Neurosci* **22**, 7055-7064 (2002).